INORGANIC CHEMISTRY
FRONTIERS

RESEARCH ARTICLE

View Article Online
View Journal | View Issue

Cite this: *Inorg. Chem. Front.*, 2020, **7**, 1386

Cooperation of cerium oxide nanoparticles and soluble molecular catalysts for alcohol oxidation†

Stephanie M. Laga, [a] Tanya M. Townsend,[a,b] Abby R. O'Connor [b] and James M. Mayer *[a]

Received 16th December 2019,
Accepted 8th February 2020

DOI: 10.1039/c9qi01640f

rsc.li/frontiers-inorganic

Cerium oxide (ceria, CeO_{2-x}) has been traditionally used as a catalyst support functionalized with metal nanoparticles or synthesized with metal dopants for a variety of applications ranging from catalytic converters to solid oxide fuel cells. In a departure from these typical heterogeneous motifs, we explore the interactions of nano-CeO_{2-x} systems with organometallic oxidation catalysts in organic solvents. Ceria is used here both as an organically-capped colloid and as an uncapped insoluble nanopowder. Both the colloid and nanopowder act as terminal oxidants by accepting hydrogen atoms from a ruthenium Noyori–Ikariya hydride complex. To our knowledge, this is the first demonstration that CeO_{2-x} can oxidize an organometallic hydride. Building on this concept, we show the uncapped CeO_{2-x} powder also acts as the terminal acceptor in catalytic alcohol dehydrogenation reactions, utilizing iridium pyridine sulfonamide catalysts under anaerobic and aerobic conditions. The coupling of homogeneous oxidation catalysts with cerium oxide demonstrates the versatility of CeO_{2-x} and a bridging of concepts in homogeneous and heterogeneous catalysis.

Introduction

There has long been interest in melding homogeneous and heterogeneous catalysis, to combine the robustness of heterogeneous catalysts with the selectivity and mechanistic understanding of homogeneous catalysts. For instance, molecular catalysts have been loosely tethered to inert supports, or activated by strong binding to a support. Homogeneous catalysts tethered to semiconductors are common in artificial photosynthetic systems, transferring photogenerated electrons or holes in the semiconductor to the surface catalyst.[1–5] Another notable example includes the development of alkane metathesis with a homogeneous alkane dehydrogenation catalyst coupled to a heterogeneous metathesis catalyst.[6,7] These are all examples of the rapidly growing field of tandem catalysis.[8–12]

Among heterogeneous catalysts, metal oxides have a long history of use, especially because of their natural occurrence, stability in air, convenient synthesis, and widespread applicability. Cerium oxide in particular has been widely used in catalysis, catalytic converters, and even biomedicine.[13] As a non-stoichiometric material, cerium oxide is typically written as CeO_{2-x} to indicate the variability in its lattice composition due to the presence of defects like oxygen vacancies that create a mixture of Ce^{3+}/Ce^{4+} sites. In three-way catalytic converters, for instance, cerium oxide provides oxygen for CO and CH oxidations and promotes NOx reduction by oxygen storage.[14] In this role, ceria stores or releases oxygen, while alumina and other precious metals act as the primary catalysts.[15,16] This application of ceria as an "active" support for other transition metal catalysts doped within the lattice or situated on the surface is typical. These heterogeneous chemical transformations between a solid support and gas phase substrates typically operate at high temperatures, sometimes exceeding 1000 °C.[17]

The use of ceria in chemical applications could be greatly expanded by developing the reactivity of the ceria in solution-based chemistry, operating at lower temperatures. In this regime, the only area that has been looked at in any detail is the use of aqueous colloidal nano-CeO_{2-x} in biomedical applications,[18–20] for example as an antioxidant to quench reactive oxygen species[21–24] or in reactions with biologically relevant reducing agents such as ascorbate or dopamine.[25,26] In a recent report by our group, colloidal cerium oxide was used in a molecular, homogeneous fashion by reaction with proton coupled electron transfer (PCET) reagents like TEMPO under mild conditions. The system was amenable to traditional homogeneous techniques, like UV-visible and ^{1}H NMR spectroscopy, to extract the $Ce^{3+/4+}$ ratio of the nanoparticles. The colloidal CeO_{2-x} exhibited extensive, reversible changes in the fraction of Ce^{3+} sites ranging from 13–67%.[27]

[a]*Department of Chemistry, Yale University, New Haven, CT 06520-8107, USA. E-mail: james.mayer@yale.edu*
[b]*Department of Chemistry, The College of New Jersey, Ewing, NJ 08628, USA*
†Electronic supplementary information (ESI) available. See DOI: 10.1039/c9qi01640f

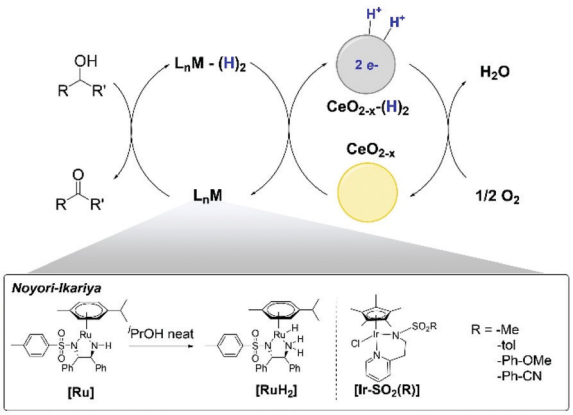

Scheme 1 Pairing of an organometallic catalyst with cerium oxide nanoparticles for alcohol dehydrogenation. An inorganic catalyst, where the L_nM form is abbreviated as [Ru] and [Ir-SO_2(R)], reacts with an alcohol to accept two hydrogen atoms. Nano cerium oxide acts as the terminal acceptor, CeO_{2-x}-$(H)_2$, in this scheme under anaerobic conditions. Oxygen may be used to oxidize ceria back to CeO_{2-x}.

This large range highlights the unique redox properties of ceria and its redox reversibility indicates its potential for use in catalysis.

Catalytic dehydrogenations have traditionally required a sacrificial H_2 acceptor, so a redox cyclable material like ceria with an affinity for protons and electrons is desirable. Olefins and ketones are typically used as the sacrificial acceptors, although acceptorless reactions can be driven at high temperatures.[28,29] Alcohol dehydrogenation was selected as the test reaction for the pairing of cerium oxide and an organometallic catalyst in this study, in part based on reports of heterogeneous ceria-supported gold or platinum systems that operate under mild conditions.[30–32] In addition to the practical interest in alcohols as a potential fuel source, a second advantage to probing alcohol dehydrogenation is the variety of homogeneous catalysts available for testing.[28]

This manuscript describes what we believe is a new approach to integrating homogeneous and heterogeneous catalysts. In these solution-based reactions, nanoscale cerium oxide (ceria) acts as a reservoir of oxidative equivalents, a hydrogen acceptor, in conjunction with homogeneous alcohol dehydrogenation catalysts. In this framework, dehydrogenation of a secondary alcohol by an organometallic catalyst L_nM forms a ketone and metal hydride $L_nM(H)_2$, which can be oxidized by cerium oxide CeO_{2-x} to regenerate the active catalyst (Scheme 1). The hydrogen-containing ceria CeO_{2-x}-$(H)_2$, is readily reoxidized with air. While the catalysis achieved in this initial example is modest, we believe that this approach has great promise, particularly for oxidation catalysis because of the stability of redox-active oxides such as ceria under oxidative conditions.

Experimental overview

To demonstrate different aspects of this alcohol dehydrogenation study three types of ceria were used: oleate-capped (olea-Ce) and oleylamine-capped (oley-Ce) cerium oxide nanoparticles (NPs) prepared according to published procedures,[33,34] as well as commercially available, uncapped cerium oxide (uc-Ce) from Strem Chemicals. TEM and powder XRD revealed the colloidal particles to be crystalline, roughly spherical, and fairly monodispersed (Fig. SI-1†). The olea-Ce have an average diameter of 3.5 nm, while the oley-Ce are slightly larger, 4.2 nm. Both types of NPs are soluble in nonpolar, aprotic solvents such as toluene, tetrahydrofuran, and cyclohexane. The commercially available Strem powder is uncapped and therefore insoluble in any solvents. It was also examined by TEM and powder XRD, d = 6.2 nm, and results were in good agreement with reported characterization data from Strem Chemicals (Fig. SI-1†). Post characterization by XRD and TEM revealed stability in the size and stability of the cerium oxide nano systems following mild redox conditions described below.

Two homogeneous catalyst systems were employed (Scheme 1). Initial studies used a commercial Noyori–Ikariya catalyst, a ruthenium complex with the (S,S)-TsDPEN ligand. This catalyst is isolable both in its oxidized purple form [Ru] and as an orange/yellow reduced hydride form [RuH_2].[35] For the [Ru] catalyst, the ready isolation of the hydride form and the distinct optical signatures of both catalytic states were critical in certain experiments discussed below (Fig. SI-2†).

Iridium catalysts containing pyridinesulfonamide ligands, developed by O'Connor *et al.*, proved to be in some ways more amenable to interfacing with nanoceria. These IrCp*(py-SO_2(R))Cl catalysts, with R = tol, Me, *p*-Ph(OMe) or *p*-Ph(CN), perform transfer hydrogenations in neat IPA at moderate temperatures and low catalyst loadings.[36,37] They also are quite temperature robust and air stable, so they were used in the aerobic catalysis experiments. Observation of hydride versions of the iridium catalysts have not been reported, but these catalysts have the advantage of not requiring base activation, simplifying the system.

Complete experimental details and additional data are given in the ESI.† Reactions with ceria were typically performed in aprotic solvents including toluene or tetrahydrofuran. Aprotic solvent was chosen in particular to facilitate the tracking of protons in this reaction. Air sensitive reactions were set up in an N_2 glovebox and run in air-free optical cuvettes and J-Young NMR tubes.

Results and discussion

Stoichiometric oxidation of a metal hydride by ceria

The key step in connecting the homogeneous oxidation catalysts with ceria is the transfer of hydrogen equivalents from the organometallic complex to the nanomaterial (Scheme 1). Hence, we monitored the reaction of the reduced (dihydride) form of the ruthenium catalyst [RuH_2] and oleylamine-capped NPs (oley-Ce), which are relatively oxidizing as-synthesized from equilibration with air.[27] In toluene at 40 °C, 1 equivalent of [RuH_2] was reacted with 4 equivalents of Ce atoms (oley-Ce)

in toluene (eqn (1)). Each oley-Ce NP contains roughly 650 Ce atoms, where *ca.* 250 ceria are on the surface of the NP (see ESI Section 2.2†). This reaction was followed by UV-visible absorption, X-ray absorption, and ^{1}H NMR spectroscopies. The cerium stoichiometry here and below is given as total Ce atoms, though only a fraction are at the surface.

$$[RuH_2] + 2Ce^{4+} \rightarrow [Ru] + 2Ce^{3+}/2H^+ \quad (1)$$

UV-visible spectroscopy of the mixture indicated the formation of the oxidized [Ru] and reduced oley-Ce. Overnight the reaction mixture changed from yellow to purple, due to the growth of an absorption feature at 550 nm (Fig. 1A). This band is due to [Ru], identified based on a comparison with independently prepared material (Fig. SI-2†). Concomitantly, the broad band-edge adsorption of CeO_{2-x} (around 340 nm) underwent a blue shift. This shift has been shown in our prior study to indicate reduction,[27] though in this case, this near-UV region of the spectrum is complicated by absorptions from the ruthenium catalysts. Control experiments with heating overnight at 40 °C showed no reaction between oley-Ce and the oxidized catalyst [Ru] and showed no conversion of $[RuH_2]$ to [Ru] in the absence of ceria (Fig. SI-3†).

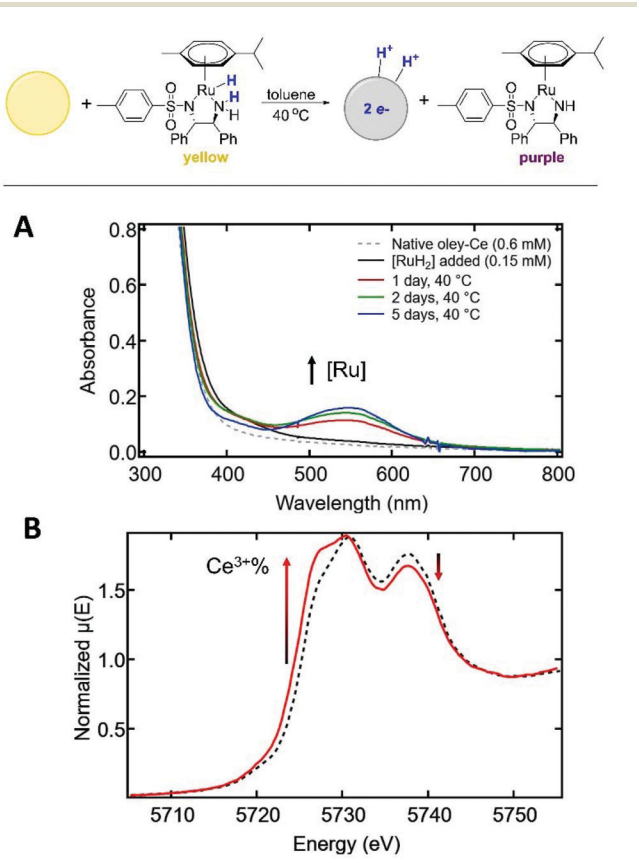

Fig. 1 (A) UV-visible spectra following the reaction of $[RuH_2]$ with oley-Ce NPs (shown at the top) in toluene at 40 °C over several days. (B) Complimentary XAS data of the hydride reaction over 24 hours (red) at the Ce–L_3 edge shows an increase of Ce^{3+}% in comparison to the native nanoparticles (black).

The oxidation state of cerium oxide was also directly probed using X-ray absorption spectroscopy (XAS). XAS is a typical method for probing changes to Ce^{3+} in mixed-valent ceria NPs. The resulting spectra can be fit according to previous literature procedures[38–40] to quantify the change in Ce^{3+}% of the NPs (see ESI section 1.2†). XAS measurements of the 24 hours reaction mixture of oley-Ce and $[RuH_2]$ at the Ce L_3 edge revealed a change of 9.7 ± 1.7% at the absorption edge indicating reduction (Fig. 1B). The stoichiometry of the reaction in eqn (1) predicts that one $[RuH_2]$ reduces two Ce atoms, so the increase in Ce^{3+}% (1.61 ± 0.28 μmoles) should correspond to 0.81 μmoles [Ru] product.

Parallel ^{1}H NMR experiments of the same XAS reaction mixture confirms the conversion of $[RuH_2]$ to [Ru] and agrees with the corresponding XAS data. Analysis of the NMR spectrum using 1,3,5-trimethoxybenzene (TMB) as an internal standard indicated 0.88 ± 0.12 μmoles [Ru] had been formed over 24 hours (Fig. SI-4†). This is within error of the expected stoichiometry (eqn (1)). In general, the former experiment and many others of colloidal oley-Ce and $[RuH_2]$ showed good mass balance; there was no major loss in the concentration of the catalyst over the reaction by NMR or UV-visible spectroscopy. Hence, data across these three spectroscopic methods suggest the clean transfer of H atoms from $[RuH_2]$ to ceria.

Colloidal suspensions of the ceria NPs always have some free capping ligand in solution, motivating control experiments to check for ligand binding to the catalyst or other processes. In our earlier survey of chemistry in this general area, the incompatibility between organically capped nanoparticles and reactive homogeneous catalysts has been a common problem (see ESI section 4.1†). No change in absorbance was observed by UV-vis spectroscopy upon addition of free oleylamine to solutions of [Ru] or $[RuH_2]$. Only free, unbound oleylamine was observed by ^{1}H NMR in a mixture of the catalyst and the ligand (Fig. SI-5†). Thus, there is no indication of any binding or reaction of the amine with the ruthenium complexes. However, the addition of oleic acid to a solution of [Ru] or $[RuH_2]$ led to immediate changes in the UV-vis absorption and ^{1}H NMR spectra that suggested ligand binding (Fig. SI-6†). This is why oley-Ce was preferred over olea-Ce in the above experiments.

The unwanted involvement of capping ligands with olea-Ce prompted us to explore similar reactivity of uncapped ceria nanopowder without ligands. As noted above, uc-Ce are insoluble and form a cloudy suspension in solution. Still, ^{1}H NMR methods were viable after centrifuging the uc-Ce to the bottom of the NMR tube. ^{1}H NMR spectra in deuterated toluene showed *ca.* 40% conversion of $[RuH_2]$ to [Ru] in the presence of 44 eq. Ce atoms after 49 hours at 40 °C (Fig. SI-7†). Further monitoring of this reaction indicated decomposition of the catalyst as the reaction progresses, with loss of the ruthenium mass balance.

Qualitatively, reactions of the solid (insoluble) NPs show visual color changes to both the catalyst solution and the solid that are indicative of hydrogen transfer. The yellow $[RuH_2]$ con-

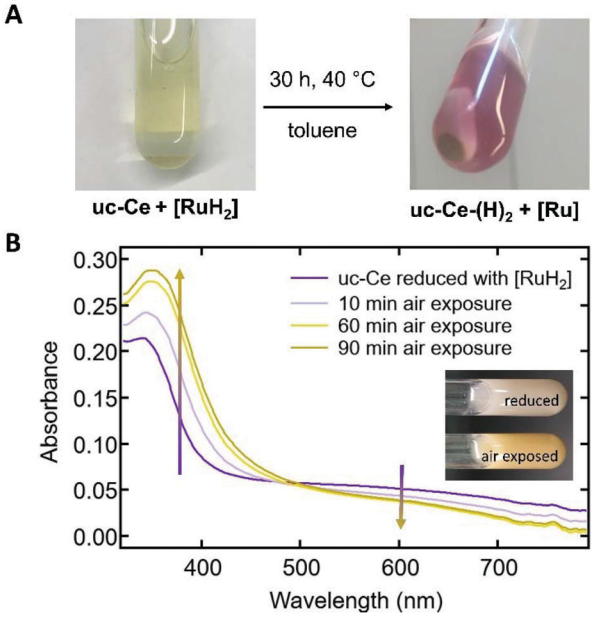

Fig. 2 (A) Reaction of uc-Ce and [RuH_2] in toluene. The yellow colored catalyst solution becomes purple as [Ru] is formed and uc-Ce becomes grayish purple in color as it is reduced. (B) UV-visible CLARiTY spectra of the uc-Ce after its isolation from the reaction mixture in A. After exposure to air with stirring, the reduced uc-Ce gradually oxidizes.

verts to the purple [Ru] in solution, and yellow uncapped ceria nanopowder (uc-Ce) becomes grey-purple (Fig. 2). UV-vis spectra of these suspensions were obtained using an OLIS CLARiTY spectrophotometer (see ESI Section 1.3 for further experimental details†).[41] Unlike a traditional UV-vis instrument, the CLARiTY contains an integrating sphere that allows measurement of the optical density of turbid samples. To account for scattering and the spherical collection cavity, correction spectra must be applied to the raw spectra to give actual absorbances. Further analysis of the uc-Ce by UV-vis (CLARiTY), confirm ceria reduction. Reduced uc-Ce, similar to colloidal NPs, has a blue shifted absorption edge and also exhibits a very broad band at around 600 nm. Upon exposure to air, this chemically reduced uc-Ce oxidizes quickly, as indicated by the red shift of the ceria absorption edge and the decrease in the broad band visible band (Fig. 2). The simple regeneration of the oxidized uc-Ce by air suggests the possibility of tandem aerobic catalysis, but such reactivity is precluded in this system by the rapid decomposition of [RuH_2] and [Ru] under air.

The studies described above show that both soluble colloidal ceria particles and insoluble ceria powder oxidize a metal dihydride by accepting an H_2 equivalent. We know of no other example of oxidation of a metal hydride complex by net H-atom transfer to an oxide surface. In contrast, a variety of studies have described related redox transfers in *derivatized* NPs: for instance the movement of reducing equivalents from a semiconductor to a platinum NP or cobaloxime catalyst[42] on the surface for hydrogen production, to a rhenium tricarbonyl catalyst for CO_2 reduction,[43] or to a ruthenium polypyridyl complex for H_2, O_2 or CO formation.[44] However, redox reactions between a NP and a molecule or catalyst are almost always described as electron (or hole) transfers. Our results in some ways parallel early reports by Grätzel *et al.* on reduction of an organometallic rhodium complex by photoreduced TiO_2, with formation of H_2.[45,46] However, this work was done in aqueous solution, where it is difficult to distinguish the movement of hydrogen atoms from separate electron and proton transfers. Like the examples described for derivatized NPs above, the reactivity was described as electron transfer from TiO_2 to the organometallic complex. The reactions described here for ceria NPs in toluene more likely involve transfer of an electron *and* proton – a hydrogen atom – between the oxide and organometallic complex.

The thermochemistry of this reaction – that hydrogen atoms transfer from [RuH_2] to the ceria NPs – is consistent with prior and ongoing work in our laboratory.[27] The mechanism of net H-atom transfer between the organometallic catalyst and the cerium oxide is not known but seems to involve a direct interaction of the homogeneous complex with the oxide surface. The alternative mechanism of H_2 loss from [RuH_2] and then reaction with ceria is unlikely because (i) there is little turnover of the catalyst for acceptorless reactions under inert atmosphere (see discussion below), arguing against the H_2 loss step, and (ii) addition of H_2 to cerium oxide typically requires elevated temperatures.[47–49]

Catalytic alcohol oxidation with ceria as the hydrogen acceptor

The role of ceria as a hydrogen acceptor in alcohol oxidations was explored following the ability of a metal hydride to transfer protons and electrons to the colloidal and uncapped ceria systems. For these studies, uncapped ceria was chosen to avoid catalyst poisoning from traditional carboxylate and amine NP capping ligands. In addition, uc-Ce may be easily separated from reaction solutions to deconvolute substrate and catalyst ^{1}H NMR and UV-vis spectra and to examine the oxidation state of cerium oxide using the CLARiTY or X-ray spectroscopic methods. However, ^{1}H NMR studies showed substantial loss of mass balance for the Noyori catalyst in the presence of uncapped ceria.

Instead, IrCp*(py-SO_2(R))Cl catalysts were explored, with R = tol, Me, *p*-Ph(OMe) or *p*-Ph(CN) ([Ir-SO_2(R)]). These iridium catalysts, reported by Ruff *et al.*, show high activity in transfer hydrogenation of acetophenone derivatives and various ketones and aldehydes without added base.[36] In addition, these catalysts were shown to operate in the presence of air, which allowed the aerobic studies described. To pick which derivative of this series to pursue, a solution of each catalyst in neat isopropyl alcohol (IPA) was heated with uc-Ce (0.35 mmol Ce atoms) at 90 °C for 12 hours. XAS analysis of the separated uc-Ce showed the most reduction for the methyl substituted catalyst (Fig. SI-8†). Based on this result, [Ir-SO_2(Me)] was selected for the catalytic studies. A control experiment, mixing a solution of [Ir-SO_2(Me)] and uc-Ce, showed less degradation, and after 87 hours *ca.* 80% of the catalyst remained in solution (Fig. SI-9†). This robustness also supported the choice of [Ir-SO_2(Me)].

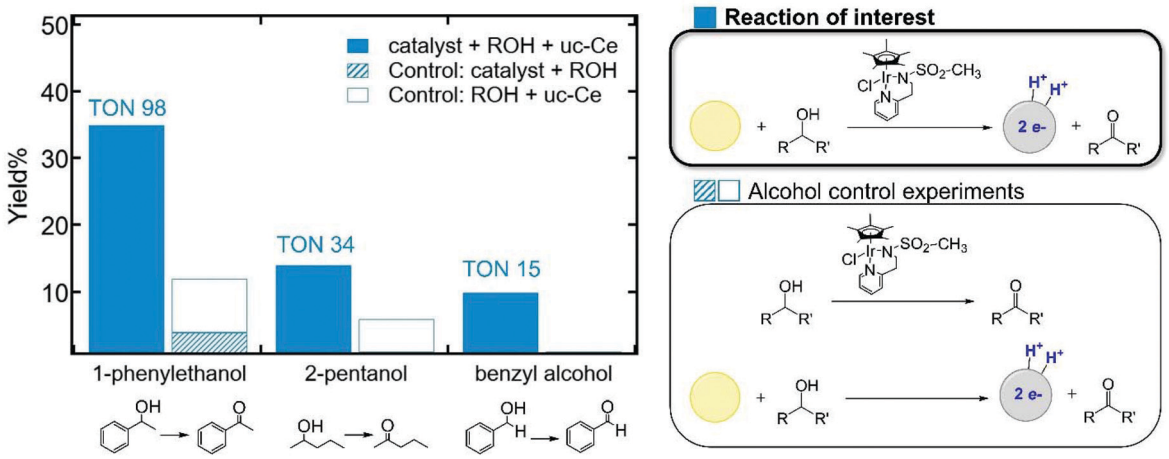

Fig. 3 Yields of ketone or aldehyde products from the catalytic oxidation and control reactions of 1-phenylethanol, 2-pentanol and benzyl alcohol. The reaction of interest (solid blue bars) utilizes the [Ir-SO_2(Me)] catalyst and uc-Ce as an acceptor under anaerobic conditions in the stoichiometry of [Ir-SO_2(Me)] : ROH : Ce atoms = 0.55 : 100 : 800. The corresponding TON for the complete catalytic reaction is given above the solid blue bar. The stripped bars correspond to the control reaction of [Ir-SO_2(Me)] and alcohol (<9 TONs for all cases), while the blank bars correspond to the control reaction of uc-Ce and alcohol. The results of the two control experiments (striped and blank bars) are stacked to show that the sum of their yields was less than those of the complete uc-Ce/[Ir-SO_2(Me)] catalytic system.

Catalytic oxidations of a series of alcohols have been surveyed using the [Ir-SO_2(Me)] catalyst and uncapped Ce nanopowder. We emphasize that in these experiments, the primary role of the ceria was as the stoichiometric terminal oxidant, not as a catalyst. These were done in toluene-d_8 to allow for quantification of the organic products by ^{1}H NMR spectroscopy using 1,3,5-trimethoxybenzene (TMB) as an internal standard (see ESI section 6.2†). The catalytic reactions were performed under a nitrogen atmosphere at 80 °C over five days in toluene with a catalytic amount of Ir using a [Ir-SO_2(Me)] : ROH : Ce atoms stoichiometry of 0.55 : 100 : 800. The observed TONs (moles of product to moles of iridium catalyst) were 16 for benzyl alcohol, 34 for 2-pentanol, and 98 for 1-phenylethanol (Fig. 3). ^{1}H NMR spectra showed conversion of 2-pentanol and 1-phenylethanol to their respective ketones and conversion of benzyl alcohol to benzaldehyde with no side products. Most likely, the [Ir-SO_2(R)] in forms a small steady-state concentration of the hydrogenated form, [Ir-SO_2(R)H_2] (eqn (2)), which transfers the two hydrogen atoms to the ceria surface. The oxidation of one substrate leads to the reduction of two Ce^{4+} sites to Ce^{3+} sites, with the addition of two protons to the ceria (eqn (3)).

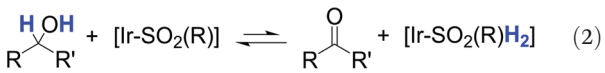

(2)

$$[\text{Ir-SO}_2(\text{R})\text{H}_2] + 2\,\text{Ce}^{4+} \longrightarrow [\text{Ir-SO}_2(\text{R})] + 2\,\text{Ce}^{3+}/\,2\,\text{H}^+ \quad (3)$$

For each alcohol, control experiments involving the removal of uc-Ce or [Ir-SO_2(Me)] from the 3-component catalytic system were also considered. The absence of uc-Ce (terminal oxidant) resulted in only 1 to 9 turnovers of the catalyst, and the absence of the Ir catalyst effected only minor amounts of oxidized product. The TONs achieved in the full catalytic system exceed the sum of the two controls (Fig. 3) and demonstrate cooperativity of [Ir-SO_2(Me)] and ceria leads to improved catalysis. Oxidations of a number of other alcohols were investigated, but these were not pursued in detail due to limited reactivity (*e.g.*, cyclohexanol) or poor mass balance (<80% for isopropanol, 4-bromo-alpha-methylbenzyl alcohol). For instance, the oxidation of isopropanol (IPA) to acetone was readily observed, but mass balance with IPA or the acetone formed was <71% at best. Likely both IPA and acetone significantly adsorb onto the surface of uc-Ce. Independent experiments simply adding acetone to a suspension of uc-Ce under these conditions showed a decrease in the solution concentration of acetone over time (Fig. SI-10†).

Aerobic oxidations with soluble iridium and uncapped ceria

The ultimate goal of connecting the chemical reactivities of a homogeneous catalyst with a heterogeneous material is to use both catalytically. In general, metal oxides are among the most robust materials for aerobic catalysis, and the [Ir-SO_2(R)] catalysts were developed to be air stable,[36] providing a good test case to explore such homogeneous/heterogeneous tandem catalysis. To move towards this goal, alcohol oxidations, with catalytic amounts of iridium, were therefore performed under aerobic conditions to allow ceria to reoxidize.

Various alcohols and catalytic [Ir-SO_2(Me)] were added to suspensions of uc-Ce in toluene-d_8 and heated for several days at 80 °C. The reactions were reopened to air at various timepoints for ^{1}H NMR spectral analysis. The same stoichiometry as in the anaerobic oxidations was used: [Ir-SO_2(Me)] : ROH : Ce atoms 0.55 : 100 : 800. As in the anaerobic reactions, the highest yields were observed when the dual ceria and catalyst system was used (refer to Fig. SI-11†). Clean conversion to a single product was still observed for 1-phenylethanol, 2-pentanol, and benzyl alcohol. The TONs were higher than under N_2, with a TON as high as 165 for 1-phenylethanol, corresponding to about a 92% yield. This is a modest but real

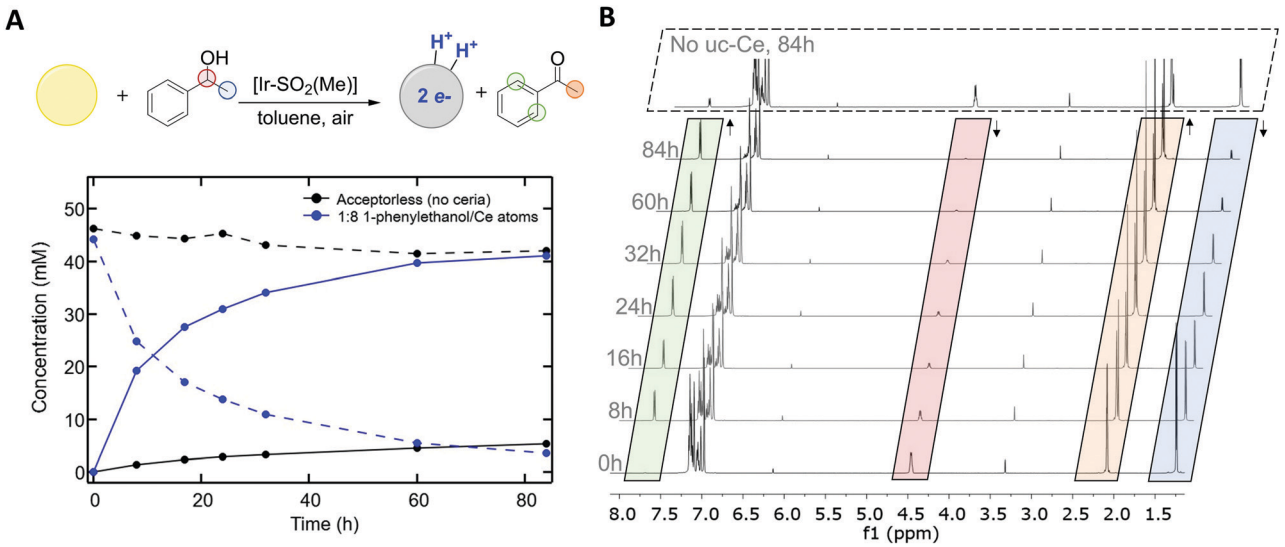

Fig. 4 Aerobic oxidation of 1-phenylethanol. (A) Plot of concentration of alcohol (dashed lines) and ketone product (solid lines) as a function of time for the full catalytic system (blue) and for the parallel control without any ceria (black). (B) ^{1}H NMR spectra of an aerobic oxidation of 1-phenyethanol with [Ir-SO_2(Me)] and uc-Ce in toluene at 80 °C. Reactions were run in a J-Young NMR tube and opened to air to replenish O_2 each time they were cooled to collect a spectrum. Spectra from 0 to 84 h of reaction time are stacked, and the top spectrum is from an independent reaction without any added uc-Ce under parallel conditions. The solid colors beneath the peaks refer to the resonances highlighted in the chemical equation.

increase over the 98 turnovers observed in the absence of O_2. The time course of this particular reaction is shown in Fig. 4. In the absence of uc-Ce, only minimal alcohol oxidation was observed with the [Ir-SO_2(Me)], as expected for an acceptorless alcohol oxidation under closed conditions.

Control experiments without catalyst showed that the direct oxidation of alcohols by uc-Ce was also enhanced by an air atmosphere. The reaction of 1-phenylethanol with suspended uc-Ce in toluene under N_2 yields only 8% 1-phenylethanone after 84 hours, but under air there is clean conversion to 71% 1-phenylethanone. In the published literature, cerium oxide is typically used as an enhancing support for a metal catalyst, rather than as the primary catalyst.[50] We have found few prior reports of ceria for alcohol oxidations reactions under such relatively low-temperature solid/solution reaction conditions. A recent report utilized cerium oxide with added hydrogen peroxide for the oxidation of benzyl alcohol.[51] Other studies use CeO_{2-x} for organic reactions,[13] such as the coupling of benzyl alcohol and aniline using CeO_{2-x} to yield the imine product, which occurs under air at 30 °C.[52]

The increase in yield we observe between N_2 and air reactions is presumably due to the ability of uc-Ce to re-oxidize under atmosphere (see Fig. 3 above). This aerobic oxidation of ROH by ceria alone makes it difficult to quantify the contribution of the organometallic catalyst when it is present. It is also difficult to quantify turnover of the ceria under the aerobic conditions because presumably only the surface of the material is active. The lack of color change of the ceria in the aerobic reactions qualitatively indicates that it is not the terminal oxidant in the alcohol oxidation, implicating a tandem catalysis scheme where ceria is also catalytic.

Additionally, the presence of dioxygen in our experiments from air exposure further complicates this question because of the possibility of soluble oxygen radical intermediates and/or radical chains. To probe this possibility, uc-Ce (0.10 mmol Ce atoms) was reacted with 9,10-dihydroanthracene (DHA) (0.02 mmol) under air at 80 °C over 4 days in toluene. The reaction yielded 42% anthracene and 3% anthraquinone as identified by ^{1}H NMR spectroscopy. Since radical-chain oxidations of DHA often give oxygenated products,[53] the low yield of the quinone suggests that the major pathway was likely not a result of reactive oxygen radicals in solution (Fig. SI-12†). Overall, these aerobic studies, along with the hydride studies and anaerobic oxidations presented above indicates that the organometallic catalyst does contribute to catalysis.

Conclusions

The cooperation between nano cerium oxide and various organometallic catalysts was explored for application to tandem catalysis. While some consideration must be given to the compatibility of the organic capping ligand for colloidal cerium oxide, we show oley-Ce acts as a homogeneous reagent and accepts H_2 from the Noyori–Ikariya ruthenium metal hydride [RuH_2]. Similarly, uncapped cerium oxide uc-Ce accepts protons and electrons from [RuH_2] and was further demonstrated to participate in catalytic alcohol oxidations using [Ir-SO_2(R)] catalysts. The nonstoichiometry of CeO_{2-x} allow it to act as a reservoir of oxidative equivalents for multi electron and proton reactivity. These reactions may be performed under inert atmosphere, but flourish when the cerium

oxide may be regenerated under air. As a recyclable acceptor, ceria has potential for further application in a tandem catalysis scheme. With the optimal organometallic catalyst and substrate pairing, cerium oxide may be utilized more effectively to target more complex organic transformations and continue bridging concepts in homogeneous and heterogeneous catalysis.

Conflicts of interest

There are no conflicts to declare.

Acknowledgements

We thank Dr Bradley McKeown and Dr Carolyn Valdez for their initial explorations in this area. This work was supported by NSF CHE-1609434 to JMM, by Yale University, and by the NSF as part of the CCI Center for Enabling New Technologies through Catalysis (CENTC), CHE-1205189. This research used resources of the X-ray Science Division Spectroscopy group (XSD-SPC) at the Advanced Photon Source, a U. S. Department of Energy (DOE) Office of Science User Facility operated for the DOE Office of Science by Argonne National Laboratory under Contract No. DE-AC02-06CH11357.

Notes and references

1 A. K. Vannucci, L. Alibabaei, M. D. Losego, J. J. Concepcion, B. Kalanyan, G. N. Parsons and T. J. Meyer, Crossing the divide between homogeneous and heterogeneous catalysis in water oxidation, *Proc. Natl. Acad. Sci. U. S. A.*, 2013, **110**, 20918.

2 Y. Zhao, K. R. Yang, Z. Wang, X. Yan, S. Cao, Y. Ye, Q. Dong, X. Zhang, J. E. Thorne, L. Jin, K. Materna, A. Trimpalis, H. Bai, S. C. Fakra, X. Zhong, P. Wang, X. Pan, J. Guo, M. Flytzani-Stephanopoulos, G. W. Brudvig, V. S. Batista and D. Wang, Stable iridium dinuclear heterogeneous catalysts supported on metal-oxide substrate for solar water oxidation, *Proc. Natl. Acad. Sci. U. S. A.*, 2018, **115**, 2902.

3 M. Wang, Y. Yang, J. Shen, J. Jiang and L. Sun, Visible-light-absorbing semiconductor/molecular catalyst hybrid photoelectrodes for H_2 or O_2 evolution: recent advances and challenges, *Sustainable Energy Fuels*, 2017, **1**, 1641.

4 T. E. Rosser, C. D. Windle and E. Reisner, Electrocatalytic and Solar-Driven CO_2 Reduction to CO with a Molecular Manganese Catalyst Immobilized on Mesoporous TiO_2, *Angew. Chem., Int. Ed.*, 2016, **55**, 7388.

5 F. Wen and C. Li, Hybrid Artificial Photosynthetic Systems Comprising Semiconductors as Light Harvesters and Biomimetic Complexes as Molecular Cocatalysts, *Acc. Chem. Res.*, 2013, **46**, 2355–2364.

6 M. C. Haibach, S. Kundu, M. Brookhart and A. S. Goldman, Alkane Metathesis by Tandem Alkane-Dehydrogenation–Olefin-Metathesis Catalysis and Related Chemistry, *Acc. Chem. Res.*, 2012, **45**, 947.

7 A. S. Goldman, A. H. Roy, Z. Huang, R. Ahuja, W. Schinski and M. Brookhart, Catalytic Alkane Metathesis by Tandem Alkane Dehydrogenation-Olefin Metathesis, *Science*, 2006, **312**, 257.

8 D. E. Fogg and E. N. dos Santos, Tandem catalysis: a taxonomy and illustrative review, *Coord. Chem. Rev.*, 2004, **248**, 2365.

9 J.-C. Wasilke, S. J. Obrey, R. T. Baker and G. C. Bazan, Concurrent Tandem Catalysis, *Chem. Rev.*, 2005, **105**, 1001.

10 P. C. Stair, Where the action is, *Nat. Chem.*, 2011, **3**, 345.

11 T. L. Lohr and T. J. Tobin, Orthogonal tandem catalysis, *Nat. Chem.*, 2015, **7**, 477.

12 Y. Yamada, C.-K. Tsung, W. Huang, Z. Huo and S. E. Habas, Nanocrystal bilayer for tandem catalysis, *Nat. Chem.*, 2011, **3**, 372.

13 T. Montini, M. Melchionna, M. Monai and P. Fornasiero, Fundamentals and Catalytic Applications of CeO_2 -Based Materials, *Chem. Rev.*, 2016, **116**, 5987.

14 A. Trovarelli, Catalytic Properties of Ceria and CeO_2-Containing Materials, *Catal. Rev.*, 1996, **38**, 439.

15 M. Cargnello, V. V. T. Doan-Nguyen, T. R. Gordon, R. E. Diaz, E. A. Stach, R. J. Gorte, P. Fornasiero and C. B. Murray, Control of Metal Nanocrystal Size Reveals Metal-Support Interface Role for Ceria Catalysts, *Science*, 2013, **341**, 771.

16 S. Bernal, J. J. Calvino, M. A. Cauqui, J. M. Gatica, C. Larese, J. A. Pérez Omil and J. M. Pintado, Some recent results on metal/support interaction effects in NM/CeO_2 catalysts, *Catal. Today*, 1999, **50**, 175.

17 L. Vivier and D. Duprez, Ceria-Based Solid Catalysts for Organic Chemistry, *ChemSusChem*, 2010, **3**, 654–678.

18 I. Celardo, J. Z. Pedersen, E. Traversa and L. Ghibelli, Pharmacological potential of cerium oxide nanoparticles, *Nanoscale*, 2011, **3**, 1411.

19 A. S. Karakoti, N. A. Monteiro-Riviere, R. Aggarwal, J. P. Davis, R. J. Narayan, W. T. Self, J. McGinnis and S. Seal, Nanoceria as antioxidant: Synthesis and biomedical applications, *JOM*, 2008, **60**, 33.

20 N. Thakur, P. Manna and J. Das, Synthesis and biomedical applications of nanoceria, a redox active nanoparticle, *J. Nanobiotechnol.*, 2019, **17**, 84.

21 A. S. Karakoti, S. Singh, J. M. Dowding, S. Seal and W. T. Self, Redox-active radical scavenging nanomaterials, *Chem. Soc. Rev.*, 2010, **39**, 4422.

22 M. Ornatska, E. Sharpe, D. Andreescu and S. Andreescu, Paper Bioassay Based on Ceria Nanoparticles as Colorimetric Probes, *Anal. Chem.*, 2011, **83**, 4273.

23 E. Sharpe, T. Frasco, D. Andreescu and S. Andreescu, Portable ceria nanoparticle-based assay for rapid detection of food antioxidants, *Analyst*, 2013, **138**, 249.

24 C. Walkey, S. Das, S. Seal, J. Erlichman, K. Heckman, L. Ghibelli, E. Traversa, J. F. McGinnis and W. T. Self, Catalytic properties and biomedical applications of cerium oxide nanoparticles, *Environ. Sci.: Nano*, 2015, **2**, 33.

25 G. Bülbül, A. Hayat, X. Liu and S. Andreescu, Reactivity of nanoceria particles exposed to biologically relevant catechol-containing molecules, *RSC Adv.*, 2016, **6**, 60007.
26 A. Hayat, D. Andreescu, G. Bulbul and S. Andreescu, Redox reactivity of cerium oxide nanoparticles against dopamine, *J. Colloid Interface Sci.*, 2014, **418**, 240.
27 D. Damatov, S. M. Laga, E. A. Mader, J. Peng, R. G. Agarwal and J. M. Mayer, Redox Reactivity of Colloidal Nanoceria and Use of Optical Spectra as an In Situ Monitor of Ce Oxidation States, *Inorg. Chem.*, 2018, **57**, 14401.
28 R. H. Crabtree, Homogeneous Transition Metal Catalysis of Acceptorless Dehydrogenative Alcohol Oxidation: Applications in Hydrogen Storage and to Heterocycle Synthesis, *Chem. Rev.*, 2017, **117**, 9228.
29 P. Pandey, I. Dutta and J. K. Bera, Acceptorless Alcohol Dehydrogenation: A Mechanistic Perspective, *Proc. Natl. Acad. Sci., India, Sect. A*, 2016, **86**, 561.
30 A. Abad, P. Concepción, A. Corma and H. García, A Collaborative Effect between Gold and a Support Induces the Selective Oxidation of Alcohols, *Angew. Chem., Int. Ed.*, 2005, **44**, 4066.
31 G. M. Mullen, E. J. Evans, I. Sabzevari, B. E. Long, K. Alhazmi, B. D. Chandler and C. B. Mullins, Water Influences the Activity and Selectivity of Ceria-Supported Gold Catalysts for Oxidative Dehydrogenation and Esterification of Ethanol, *ACS Catal.*, 2016, 1216–1226.
32 H. Wang, K. An, A. Sapi, F. Liu and G. A. Somorjai, Effects of Nanoparticle Size and Metal/Support Interactions in Pt-Catalyzed Methanol Oxidation Reactions in Gas and Liquid Phases, *Catal. Lett.*, 2014, **144**, 1930.
33 T. Yu, J. Joo, Y. I. Park and T. Hyeon, Large-Scale Nonhydrolytic Sol–Gel Synthesis of Uniform-Sized Ceria Nanocrystals with Spherical, Wire, and Tadpole Shapes, *Angew. Chem., Int. Ed.*, 2005, **44**, 7411.
34 T. Taniguchi, T. Watanabe, N. Sakamoto, N. Matsushita and M. Yoshimura, , Aqueous Route to Size-Controlled and Doped Organophilic Ceria Nanocrystals, *Cryst. Growth Des.*, 2008, **8**, 3725.
35 K.-J. Haack, S. Hashiguchi, A. Fujii, T. Ikariya and R. Noyori, The Catalyst Precursor, Catalyst, and Intermediate in the RuII-Promoted Asymmetric Hydrogen Transfer between Alcohols and Ketones, *Angew. Chem., Int. Ed. Engl.*, 1997, **36**, 285.
36 A. Ruff, C. Kirby, B. C. Chan and A. R. O'Connor, Base-Free Transfer Hydrogenation of Ketones Using Cp*Ir(pyridinesulfonamide)Cl Precatalysts, *Organometallics*, 2016, **35**, 327–335.
37 T. M. Townsend, C. Kirby, A. Ruff and A. R. O'Connor, Transfer hydrogenation of aromatic and linear aldehydes catalyzed using Cp*Ir(pyridinesulfonamide)Cl complexes under base-free conditions, *J. Organomet. Chem.*, 2017, **843**, 7.
38 A. M. Shahin, F. Grandjean, G. J. Long and T. P. Schuman, Cerium LIII-Edge XAS Investigation of the Structure of Crystalline and Amorphous Cerium Oxides, *Chem. Mater.*, 2005, **17**, 315.
39 P. Nachimuthu, W.-C. Shih, R.-S. Liu, L.-Y. Jang and J.-M. Chen, The Study of Nanocrystalline Cerium Oxide by X-Ray Absorption Spectroscopy, *J. Solid State Chem.*, 2000, **149**, 408.
40 M. I. B. Bernardi, A. Mesquita, F. Béron, K. R. Pirota, A. O. de Zevallos, A. C. Doriguetto and H. B. de Carvalho, The role of oxygen vacancies and their location in the magnetic properties of $Ce_{1-x}Cu_xO_{2-\delta}$ nanorods, *Phys. Chem. Chem. Phys.*, 2015, **17**, 3072.
41 Clarity Spectrophotometers, OLIS, Inc. United States, https://www.olisclarity.com/, (accessed November 2019).
42 J. L. Dempsey, J. R. Winkler and H. B. Gray, Kinetics of Electron Transfer Reactions of H_2 -Evolving Cobalt Diglyoxime Catalysts, *J. Am. Chem. Soc.*, 2010, **132**, 1060.
43 M. Abdellah, A. M. El-Zohry, L. J. Antila, C. D. Windle, E. Reisner and L. Hammarström, Time-Resolved IR Spectroscopy Reveals a Mechanism with TiO_2 as a Reversible Electron Acceptor in a TiO_2–Re Catalyst System for CO_2 Photoreduction, *J. Am. Chem. Soc.*, 2017, **139**, 1226.
44 T.-T. Li, B. Shan, W. Xu and T. J. Meyer, Electrocatalytic CO_2 Reduction with a Ruthenium Catalyst in Solution and on Nanocrystalline TiO_2, *ChemSusChem*, 2019, **12**, 2402.
45 U. Kölle and M. Grätzel, Organometallic Rhodium(III) Complexes as Catalysts for the Photoreduction of Protons to Hydrogen on Colloidal TiO_2, *Angew. Chem., Int. Ed. Engl.*, 1987, **26**, 567.
46 P. Cuendet, K. K. Rao, M. Grätzel and D. O. Hall, Light induced H_2 evolution in a hydrogenase-TiO_2 particle system by direct electron transfer or via Rhodium complexes, *Biochimie*, 1986, **68**, 217.
47 S. Bernal, J. J. Calvino, G. A. Cifredo, J. M. Gatica, J. A. P. Omil and J. M. Pintado, Hydrogen chemisorption on ceria: influence of the oxide surface area and degree of reduction, *J. Chem. Soc., Faraday Trans.*, 1993, **89**, 3499.
48 S. Bernal, J. J. Calving, G. A. Cifredo, J. M. Rodríguez-Izquierdo, V. Perrichon and A. Laachir, Reversibility of hydrogen chemisorption on a ceria-supported rhodium catalyst, *J. Catal.*, 1992, **137**, 1.
49 J. L. G. Fierro, J. Soria, J. Sanz and J. M. Rojo, Induced changes in ceria by thermal treatments under vacuum or hydrogen, *J. Solid State Chem.*, 1987, **66**, 154.
50 M. Alhumaimess, Z. Lin, W. Weng, N. Dimitratos, N. F. Dummer, S. H. Taylor, J. K. Bartley, C. J. Kiely and G. J. Hutchings, Oxidation of Benzyl Alcohol by using Gold Nanoparticles Supported on Ceria Foam, *ChemSusChem*, 2012, **5**, 125.
51 P. Tamizhdurai, S. Sakthinathan, S.-M. Chen, K. Shanthi, S. Sivasanker and P. Sangeetha, Environmentally friendly synthesis of CeO_2 nanoparticles for the catalytic oxidation of benzyl alcohol to benzaldehyde and selective detection of nitrite, *Sci. Rep.*, 2017, **7**, 46372.
52 M. Tamura and K. Tomishige, Redox Properties of CeO_2 at Low Temperature: The Direct Synthesis of Imines from Alcohol and Amine, *Angew. Chem., Int. Ed.*, 2015, **54**, 864.
53 United States, US3642838A, 1972.